

## **MODELING OF BATHYMETRY FOR LAKE MANZALA USING REMOTE SENSING AND GIS**

Rana E. Elshazly<sup>1</sup>, Mohamed M. Elshemy<sup>2&3</sup>, Bakenaz. A. Zeidan<sup>4</sup>, Asaad M. Armanuos<sup>5</sup>

<sup>1,2,4,5</sup> Faculty of Engineering, Tanta University, 31511 Tanta, Egypt

<sup>3</sup> Faculty of Engineering, Al-Baha University, Al-Baha, KSA

<sup>1</sup> E-mail: [rana.elshazli@f-eng.tanta.edu.eg](mailto:rana.elshazli@f-eng.tanta.edu.eg)

<sup>2</sup> E-mail: [m.elshemy@f-eng.tanta.edu.eg](mailto:m.elshemy@f-eng.tanta.edu.eg)

<sup>4</sup> E-mail: [b.zeidan@f-eng.tanta.edu.eg](mailto:b.zeidan@f-eng.tanta.edu.eg)

<sup>5</sup> E-mail: [asaad.matter@f-eng.tanta.edu.eg](mailto:asaad.matter@f-eng.tanta.edu.eg)

### **ABSTRACT**

Lake Manzala is a brackish lake in northeastern Egypt on the Nile Delta near Port Said. It is the largest of the northern deltaic lakes of Egypt along the Mediterranean coast. It has changes in the water body due to the severe anthropogenic activities. It has an economic value in addition to environmental impacts on the nearby society. Bathymetry is one of the important marine geospatial data which is used in many hydrographic analyses. Landsat 8 imagery with a resolution of 30 m is utilized for satellite derived bathymetry (SDB). Generalized Linear Model (GLM) and GIS software are used in this study for processing of the images and managing the database of each image. The visible electromagnetic spectrum reflectance intensity determines various depths due to attenuation processes. This research focuses on fast and practical bathymetry modeling of Lake Manzala using GLM. At first, Landsat imagery is corrected for the atmospheric conditions and sun glint effect. And then, values from the logarithms of corrected reflectance bands "coastal, blue, green and red" and their ratio logarithms at the corresponding locations of GPS survey were extracted. Two typical regions in the lake are considered: shallow zone (max. depth of 1.61 m) and deep zone (max. depth of 7.95 m). Two statistical indices, Root Mean Square Error (RMSE) and correlation (R) are used to calibrate the logarithms derived values of the model using observed data for the lake. The results show a good performance of GLM. RMSE values are 0.607 m and 0.126 m, while R values are 0.813 and 0.532, for deep and shallow regions, respectively. Based on this work, the lake bathymetry may be derived for modeling studies with an acceptable resolution. This methodology is recommended for shallow lakes, which saves monitoring cost.

**Keywords:** ArcGIS, Bathymetry, Generalized Linear Model, Lake Manzala, Landsat, Remote Sensing

### **1 INTRODUCTION**

Modeling the lake bathymetry is one of the important parameters for various applications of marine studies; maps, planning and management. Bathymetry has a fundamental effect on energy conversion, safe navigation, and spatial variability in surf zone circulation and sediment transportation in coastal zones. Lake Manzala is the largest lake of northern Egyptian lakes and the most productive for fisheries (Zahran et al.2015). Bathymetric maps are often difficult to obtain by the conventional method of depth extraction using shipboard echo-sounders, due to need experience, time and cost (Ieu and change 2005, Patel et al. 2015). The theory behind the bathymetry from remote sensing is that different wavelengths of light penetrate water with varying degrees which the light passes through water becomes attenuated by interaction with water column according to Beers Law (Ehse & Rooney 2015 and Green et al. 2000). To obtain water depths, the techniques which are modeling through a statistical relationship between image pixel values and in-situ data are applied (Makboul et al. 2018). Therefore, the light is reflected from seabed as a bright in shallow areas which as a less amount of light has been absorbed. Conversely, deep areas appear darker (Melsheimer and Chin 2001).

In 2003, Stumpf et al. proposed a ratio algorithm (blue/green) bands reflectance to determine the depth of water based on the difference in attenuation properties between bands. Therefore, the effects of different heterogeneous water areas were assumed the same for two bands and so the ratio between their reflectance values to detect water depths. Then in 2008, Su et al. used various algorithms for estimating water depths from optical satellite images depending on the relationship between image pixel values and water depths samples. To avoid defects of the Stumpf's theory, the authors tried to calibrate parameters for the non-linear inversion model automatically using the Levenberg-Marquardt optimizing algorithm. Gholamalifard et al. 2013 tested three different methods for extracting bathymetry from Landsat 5 satellite in the southeastern Caspian Sea, Iran. Single band algorithm (SBA) utilizing either blue or red bands, principal components analysis (PCA) and multi-layer perception (back propagation) neural network between visible bands (MLP-ANN). The MLP-ANNs method produced the best depth estimates. The single band algorithm utilizing a red band also produced reasonably accurate results while blue band algorithm and PCA didn't perform. In 2015, Jagalingam et al. made attempt to determine the bathymetry of the southwest coast of India by applying the ratio transform algorithm on the blue and green bands of landsat-8 satellite image. The study computed between the logarithm values and the hydrographic chart sounding values, by using this tool a good correlation in deep area. Poppenga et al. 2018 applied the band ratio technique to Landsat 8 and World View-3 for shallow near-shore on Majuro Atoll, the Landsat 8 derived SDB estimates from the blue/green ratio had ( $R^2 = 0.9324$ ) and from the Coastal/red band ratio had ( $R^2 = 0.9597$ ), SDB estimates derived from world view-3 imagery exhibited an ( $R^2 = 0.9574$ ).

Abayazid 2017 applied three techniques for satellite based water depth retrieval; artificial neural network (ANN), single band algorithm (SBA) and multi-band ratio transform model using Landsat 8 in the Nile Delta coast, Egypt. Training alternative ANN showed moderate correlation. On other hand; SBA showed poor performance and optimum derivation of satellite for ratio transform technique. In 2017, Negm et al. aimed to assess the performance of generalized linear model (GLM), 3<sup>rd</sup> order polynomial and artificial neural network (ANN) to determine the bathymetry at a part of Rosetta branch of the Nile River, Egypt, using Landsat 8. The green band logarithm was applied to the 3<sup>rd</sup> order polynomial, (coastal, blue, green, red) bands algorithms to GLM, visible bands are used as an input layer to neural network. The ANN model was more accurate than other models. However; results of the three models weren't satisfactory due to the high turbidity. Mohamed et al. 2017 assessed the performance of three proposed empirical models: the ensemble regression tree-fitting algorithm using bagging (BAG), ensemble regression tree-fitting algorithm of least squares boosting (LSB) and support vector regression algorithm (SVR) in three different areas: Alexandria (Egypt), lake Nubia (Sudan) and Shiraho (Ishigaki Island, Japan). Landsat-8 and Spot-6 satellite images were used. The three models used the reflectance of green, red, blue/red and green/red band ratios which were compared with the neural network (ANN) and Generalized Linear Model (GLM). BAG, LSB and SVR had higher accuracy than GLM and ANN. The BAG algorithm was the most accurate for bathymetry calculations. Elshahi et al. 2018 used multiple linear regression for logarithms of reflectance bands to estimate bathymetry of the Aswan High Dam Reservoir, Egypt. The authors quantified the error between in-situ measurements and Landsat 8 estimated depth values. The results showed that the multiple regression method has better good predicting depths from 20 to 25 m and lower predicting to the depth from 8 to 20 m.

The objective of this research is to apply a methodology for modeling the bathymetry of Lake Manzala using Landsat 8 multiband combination after removing distortions resulting from atmospheric and sun-glint effects. The values from the logarithms of corrected reflectance bands and their ratio logarithms at the corresponding locations of GPS survey will be used to obtain bathymetric maps by applying generalized linear model (GLM).

## 2 MATERIALS AND METHODS

### 2.1 Study area and Data collection

The study area which is selected for modeling shallow lakes bathymetry in Egypt is Lake Manzala. Lake Manzala is the largest brackish lake in the north of Egypt along the Mediterranean coast (Donia and Farag 2012) as shown in Fig.1. Geographically, it is located between longitudes  $31^{\circ} 45'$  and  $32^{\circ} 22'$  E and latitudes  $31^{\circ} 00'$  and  $31^{\circ} 35'$ . The lake is bounded by the Suez Canal to the east, the Mediterranean Sea to the north and northeast, Dakahlia and Sharkia provinces to the south, and Nile-Damietta branch to the west (Zahran et al. 2015). It has a maximum length of 64.5 km, a maximum width of 49 km, and a total shoreline length of 293 km. The lake area approximately  $1031 \text{ km}^2$  (El-Asmar and Hereher 2011). It has changes in the water body due to the severe anthropogenic activities. It is connected to six drains. The lake depth ranges from 0.5 to 8.0 m. However, it is a shallow lagoon where more than 50% of the lake area has a depth ranged between 1.0 and 1.4 m (Thompson et al. 2009). The deep depths are not dominate. In-situ depth measurements for two years 2013-2014 were supplied from the surveys of MELMARINA Primary Lagoons Project which employed a Lawrence GPS/echo sounder system deployed from a fiber glass boat.

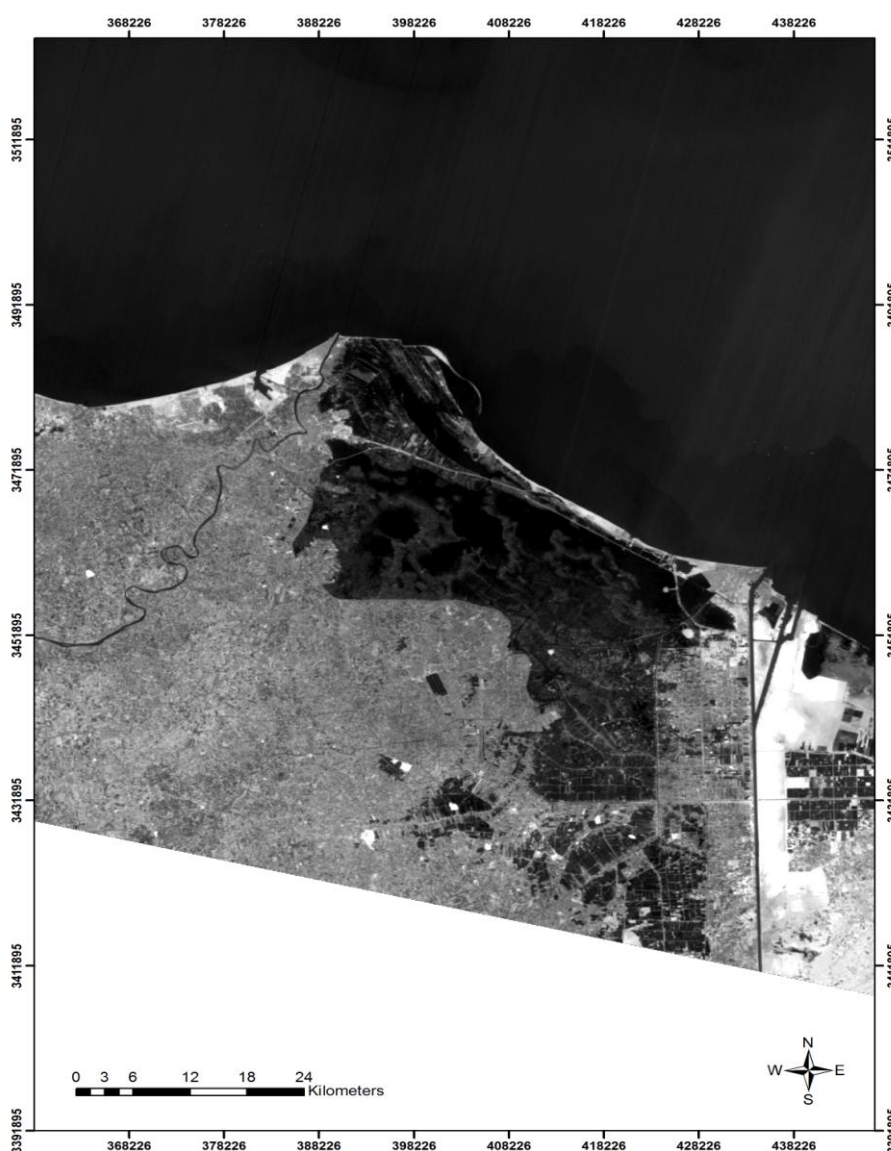


Figure1 . Landsat 8 image of the study area (Lake Manzala), source : <https://earthexplorer.usgs.gov/>

## 2.2 Satellite Image and Sensor Data

Landsat 8 imagery data collects 11 spectral bands with a spatial resolution 30m. The bands used for determining bathymetry are band 1 coastal/aerosol (0.435-0.451  $\mu\text{m}$ ), band 2 blue (0.452-0.512 $\mu\text{m}$ ), band 3 green (0.533-0.590  $\mu\text{m}$ ), band 4 red (0.636-0.673  $\mu\text{m}$ ) and band 5 near-infrared (NIR) (0.851-0.879  $\mu\text{m}$ ), Landsat 8 (L8) Data Users Handbook. Landsat 8 imagery is freely available and all imageries are referenced to WGS84 datum. The Landsat 8 imagery used in this study was downloaded from the earth explorer USGS in level 1 Geotiff (systematic correction) product on (25-10-2014) with an average cloud cover less than 10% with metadata files required for radiometric image corrections.

## 3 METHODOLOGY

Environmental factors effect on satellite image such as atmosphere and sun specular reflection. It needs correcting to avoid the influence of the inversion depth. The pre-processing is an important stage to improve the precision of inversion depth. Firstly, the radiometric pixel values are converted to spectral reflectance (Todd and Chris 2010). Secondly, atmospheric correction is applied to the image .Thirdly, water reflectance values are separated from the land and applying sun de-glint correction to decrease noise on the input image (Doxani et al. 2012). The logarithm reflectance corrected values corresponding to in-situ depth measurements are extracted from multispectral images for usage bands. The methodology is summarized according to the flow chart in Fig. 2.

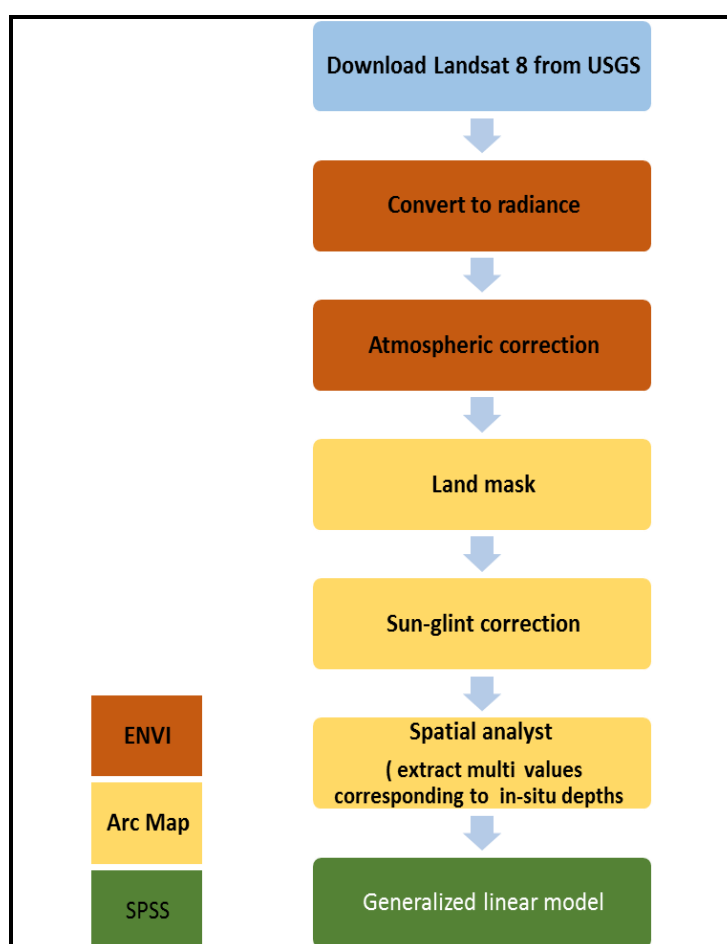


Figure 2. Flow chart showing the methodology adopted in this study and the used software.

### 3.1 Converting to Radiance

Converting of the digital number (DN) to the spectral radiance at the aperture ( $L_\lambda$ ) is done using the following equation:

$$L_\lambda = ML \times Q_{cal} + AL \quad (1)$$

Where:

$L_\lambda$  = Spectral radiance ( $W / (m^2 * sr * \mu m)$ ),

ML = Radiance multiplicative scaling factor for the band (RADIANCE\_MULT\_BAND\_n from the metadata),

AL = Radiance additive scaling factor for the band (RADIANCE\_ADD\_BAND\_n from the metadata), and

$Q_{cal} = L_1$  pixel value in DN (Landsat 8 (L8) Data Users Handbook)

### 3.2 Atmospheric Correction

An important step in remote sensing is to correct atmospheric effects. Solar radiation which reflected by the earth's surface to satellite sensors is modified by its interaction with the atmosphere. Therefore, images effected by several factors such as distribution of aerosols, water vapor and visibility. The FLAASH model in ENVI software is used for atmospheric correction and it's based on the MODTRAN4 radiation transfer code (Berk et al. 1998). The input image must be radiometrically calibrated radiance image and data in floating point format before using FLAASH model in ENVI software. FLAASH needs information on the geographical center location of the image and the time it was captured. This information can't be retrieved automatically from the data file, but must be entered by the user. An atmospheric model must be selected depending on climate (latitude and time of year). Urban aerosol model is selected depending on the expected type of aerosols and visibility present. FLAASH starts according to the following for spectral radiance at a sensor pixel (ENVI 2009).

$$L = \left( \frac{A\rho}{1 - \rho_e S} \right) + \left( \frac{B\rho}{1 - \rho_e S} \right) + L_a \quad (2)$$

Where:

$\rho$  is the pixel surface reflectance,

$\rho_e$  is an average surface reflectance for the pixels and a surrounding region,

S is the spherical albedo of the atmosphere,

$L_a$  is radiance back scattered by atmosphere, and

A and B are coefficients that depended on atmospheric and geometric conditions but not on the surface.

Moreover A, B, S and  $L_a$  are depending on water vapor amount.

### 3.3 Land Mask

When extracting aquatic information, it is important to mask out land features from image. The reflectance values of the NIR band are used to separate water from land as a result of the appearance of land in bright and water in dark (Pushparaj and Hegde 2017). By using ArcGIS the land/water threshold value was calculated by drawing a line from land (bright area) to water (dark area). The threshold value is used to separate water for the following application to the coastal/aerosol, blue, green and red bands, (The IHO-IOC GEBCO Cook Book 2018).

### 3.4 Sun Glint Correction

For accurate benthic habitat classification, the specular reflection of solar radiation, known as sun glint must be removed. This problem was overcome by (Hochberg et al. 2003) who used an effective method to remove the sun glint by utilization of the brightness in (NIR) band. Hedley revised this method by using the linear relationships between (NIR) band and visible bands based on a sample of the image pixels. All the selected pixels for each visible band are included in a linear regression of NIR brightness (x-axis) against the visible band brightness (y-axis), (Hedley et al. 2005). All pixels in the image for band  $i$  (visible bands) can be de-glinted by applying the following equation:

$$R'_i = R_i - b_i \times (R_{NIR} - \text{Min}_{NIR}) \quad (3)$$

Where:

$R'_i$  the sun-glint corrected pixels in band  $i$ ,

$(b_i)$  the product regression slope and,

$R_{NIR}$  corresponding pixel value in NIR band and  $\text{Min}_{NIR}$  is the min NIR value existing in the sample.

By using ArcGIS, the equation is applied on the atmospherically corrected reflectance (coastal/aerosol, blue, green and red) bands and the (NIR) band.

### 3.5 Statistical Model

#### 3.1.5 Generalized linear model

The most common method for deriving SDB from passive satellite imagery is the generalized linear model (GLM). The GLM is based on the difference in absorption rates between the logarithms of bands used for bathymetry and single logarithms of bands. To overcome the weak relationship of single band, which assumed that the bottom surface is homogenous and water column is uniform, Lyzenga et al. (1985) used a ratio of two bands to correct these demerits. The reflectance values of band with a higher absorption rate will decrease proportionally faster than the reflectance values of band with a lower absorption rate, as the depth increases. Furthermore, Lyzenga et al. (2006) generalized this approach that it gives water depths not influenced by the water column and bottom type. The bathymetry can be calculated using the following equation (lyzenga et al. 2006):

$$Z = a_0 + \sum_{i=1}^N a_i X_i \quad (4)$$

Where:

$Z$  is the water depth,

$a_0$  and  $a_i$  are coefficients determined through multiple regression using the reflectance of the corresponding bands and the known depth, and

$X_i$  is the logarithm of corrected bands.

Recently, Mohamed et al. (2017) and Sánchez-Carnero et al. (2014) used a GLM to a linear combination of the single logarithm of corrected bands and their ratio. The GLM represents the least-squares fit of the link of the response to the data (Negm et al. 2017). By using the link function of  $(g [\mu Y])$ , the observed non-linear variable can be fitted to a linear predictor of the explanatory variables as in the following equation (Sánchez-Carnero et al. 2014):

$$g [\mu Y] = \beta_0 + \sum_i \beta_i X_i + \sum_{ij} \beta_{ij} X_i X_j \quad (5)$$

Where,  $\beta_0$ ,  $\beta_i$ , and  $\beta_{ij}$  are coefficients and  $X_i$  and  $X_j$  are variables

## 4 RESULTS

The Landsat 8 image of the study area is pre-processed for estimating the bathymetry by converting the image pixel values to radiance utilizing the image metadata file values using ENVI 5.1 and performing atmospheric correction using FLAASH tool, with the input parameters set as described in the methodology. Moreover, ArcGIS 10.2 environment is used for separating the land from water, the threshold value is estimated from the NIR band as shown in Fig.3, which indicates the smooth section with low values representing water, whereas the fluctuating high values represent land. Thus, the threshold value 0.025m is applied on the coastal, blue, green and red bands to separate water from land. And also correcting sun-glint as the recommendations of (Hedley et al. 2005) by using ArcGIS is shown in Fig.4.

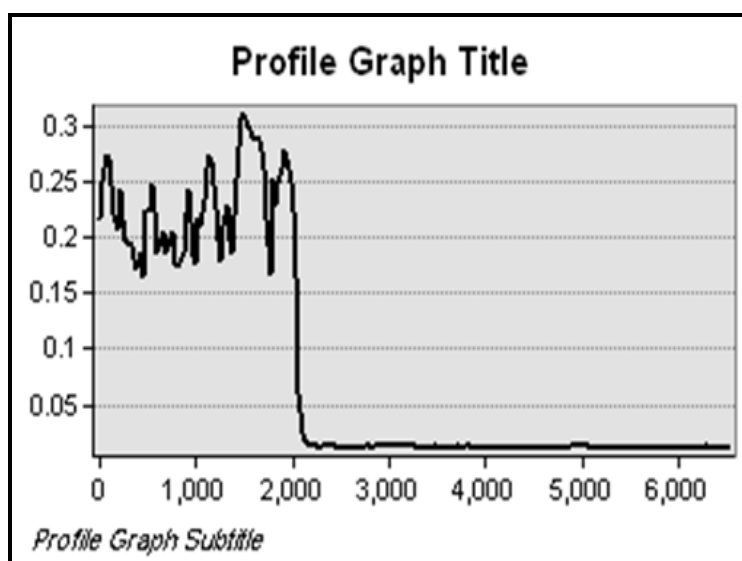
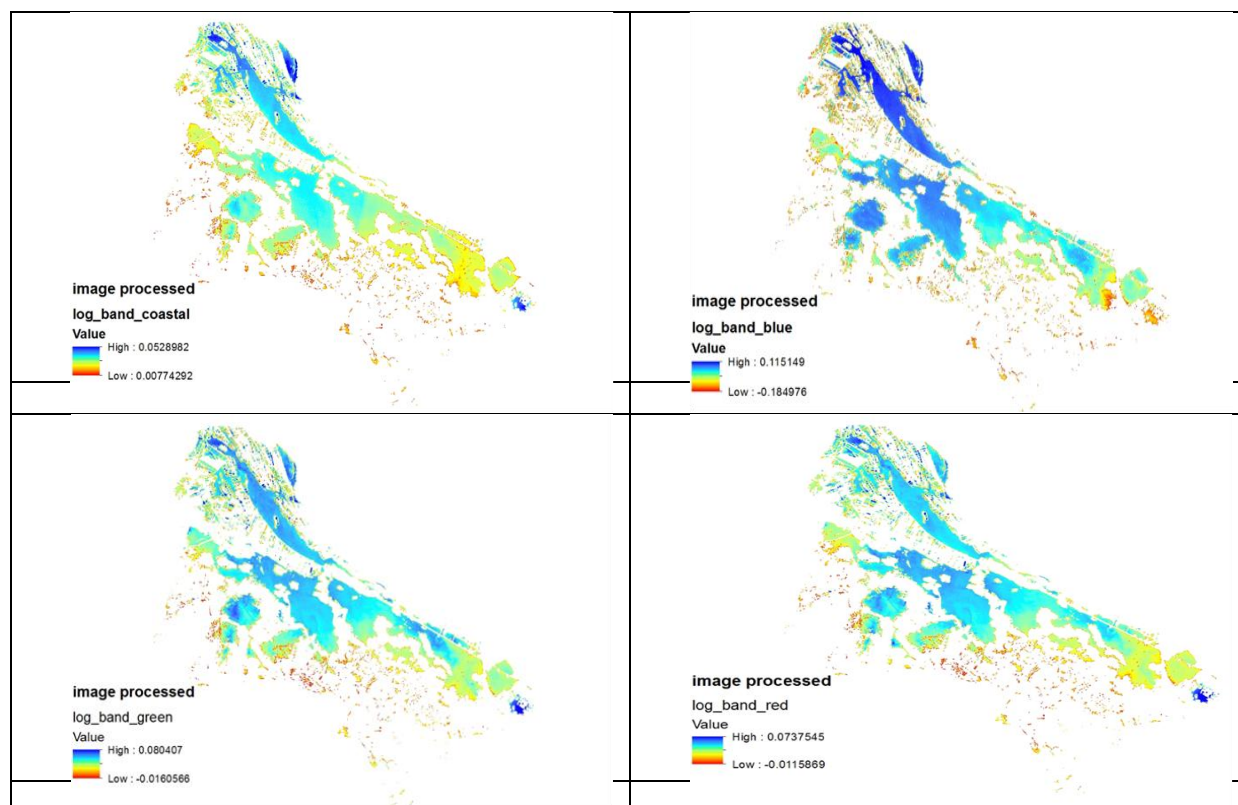


Figure 3. the threshold value to separate the land from water



**Figure4. Landsat 8 bathymetry for lake Manzala, a: the bathymetry of coastal band, b: the bathymetry of blue band, c: the bathymetry of green band and d: the bathymetry of red band.**

The input values for training algorithms were extracted from the corrected reflectance images at the corresponding locations of the echo sounder field points. Ten inputs are used for training GLM approach: the values of coastal, blue, green, red, coastal/blue, coastal/green, coastal/red, blue/green, blue/red and green/red bands logarithms using ArcGIS and export data as type dBASE Table.

The generalized linear model is carried out in SPSS v20 to calculate the coefficients of model and determine which of bands logarithms and their ratio giving the best correlation. Two typical regions in the lake were considered; Shallow zone and deep zone. Which results of SPSS show coastal, blue, green, coastal/green, and blue/green more effective for deep zone, where the depth can be derived by applying the equation (6):

$$Z_{\text{deep}} = -264.946 + (25 \times B_{23}) + (225.15 \times B_{13}) - (74.74 \times B_3) + (7.304 \times B_2) + (62.818 \times B_1) \quad (6)$$

Where:

$B_3, B_2, B_1$  are the logarithms of the corrected reflectance of green, blue and coastal &  $B_{23}, B_{13}$  are logarithm ratio values of blue/green and coastal/green.

The coefficient of determination  $R^2$  and RMSE was calculated to evaluate the model; ( $R^2 = 0.66$ ) & (RMSE = 0.607m).

For the shallow zone blue, red, coastal/green, and green/red, the depth can be derived by applying the equation (7):

$$Z_{\text{shallow}} = -11.325 + (1.97 \times 10^{-5} \times B_2 - (2.102 \times B_4) + (3.92 \times B_{13}) + (1.15 \times B_{34}) \quad (7)$$

Where:

$B_2$ ,  $B_4$  are the logarithms of the corrected reflectance of blue and red &  $B_{13}$ ,  $B_{34}$  logarithm ratio values of coastal/green and green/red.

The coefficient of determination  $R^2$  and RMSE was calculated to evaluate the model; ( $R^2 = 0.283$ ) & (RMSE = 0.126m).

## DISCUSSION

In this research, a procedure was evolved to model the bathymetry of Lake Manzala using the Landsat-8 satellite imagery. It is important to pre-process the satellite image before estimating the bathymetry. Therefore, the two corrections of atmospheric and sun glint were applied on the reflectance image. The selection of appropriate bands for bathymetry was performed through a statistical analysis to investigate the correlation between water depth and the visible logarithm bands and their ratio. The generalized linear model correlates the bands combination directly to water depth. The search for the best combination of the selected bands is performed through SPSS software based on the lowest value of root mean square error and the highest correlation. The correlation between derived depth and in-situ depth values obtained for bands combinations as shown in Fig. 5. The results show a good correlation ( $R = 0.813$ ) and RMSE (0.607m) for deep zone and ( $R = 0.532$ ) & (RMSE = 0.126m) for shallow zone.

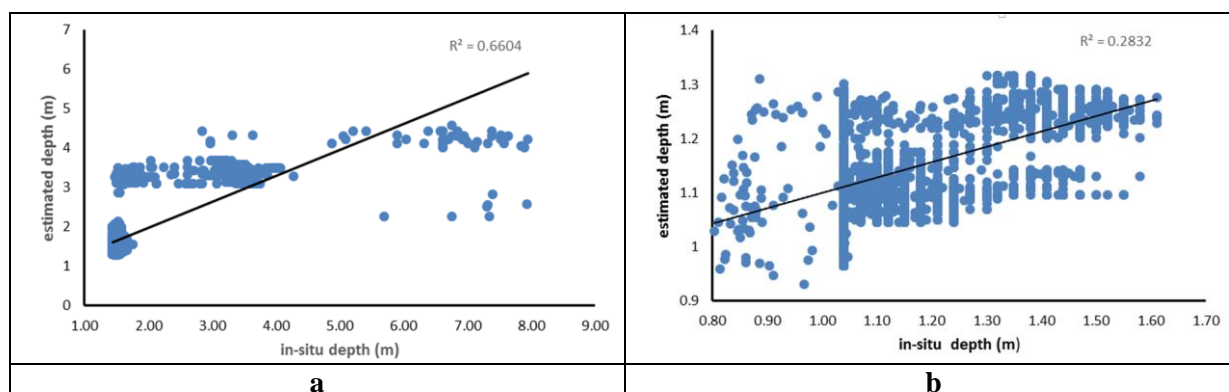


Figure 5. The GLM continuous fitted model. Line represents the fitted continuous model while depths are represented as points: a) deep zone & b) shallow zone.

## 5 CONCLUSIONS & RECOMMENDATIONS

Modeling bathymetry for shallow coastal lake areas is essential for hydrological engineering applications such as sedimentary processes and coastal studies (Mohamed et al. 2017). Approaches of remotely sensed bathymetry algorithm are principally based on empirical relationship link radiance in multispectral imagery with ground truth, and are acknowledged to be site specific and non-transferable to other region (Abayazid HO 2017). This research study aimed to model bathymetry for Manzala Lake using freely available Landsat 8 imageries. The bathymetry is estimated as the proposed methodology used visible bands corrected from atmospheric and sun-glint errors and their logarithms as input values. Generalized linear model has been applied using processed imagery in correspondence with in-situ measurements. Results obtained from GLM using coastal, blue, green and red logarithm bands and band combinations indicated best depth retrieval by training band the logarithms of the corrected reflectance of green, blue and coastal and logarithm ratio values of blue/green and coastal/green for deep zone. And training band the logarithms of the corrected reflectance of blue and red and coastal and logarithm ratio values of coastal/green and green/red for shallow zone. Results proved the advantageous capability of deriving satellite imagery-based bathymetry of Lake Manzala with satisfactory performance. Where, RMSE is about (0.607, 0.126) m,

while R is (0.813, 0.532) for deep and shallow zones, respectively. Based on this work, the lake bathymetry may be derived for modeling studies with an acceptable resolution.

## REFERENCES

Abayazid, H.O. (2017), "Comparative Assessment of Techniques for Bathymetry Derivation from Multi Spectral Satellite Imagery in the Nile Delta Coast-Egypt", *Journal of scientific and Engineering Research*, 4(3):69-78

Berk A, Bernstein L, Anderson G, Acharya P, Robertson D, Chetwynd J, Adler S (1998), "MODTRAN cloud and multiple scattering upgrades with application to AVIRIS", *Remote Sens Environ* 65(3):367–375. Doi: 10.1016/S0034-4257(98)00045-5

Donia N, Farag H (2012) Monitoring Burullus Lake using remote sensing techniques. Sixteenth International Water Technology Conference, IWTC 16 2012, Istanbul, Turkey

Doxani G, Papadopoulou M, Lafazani P, Pikridas C, Tsakiri M (2012), "Shallow-water bathymetry over variable bottom types using multispectral Worldview-2 image", *ISPRS – Int Arch Photogramm, Remote Sens Spat Inf Sci XXXIX-B8:159–164*. [Doi: 10.5194/isprsarchives-XXXIX-B8-159-2012](https://doi.org/10.5194/isprsarchives-XXXIX-B8-159-2012)

Ehse, J.S. and Rooney, J. J. (2015). Depth Derivation Using Multispectral WorldView-2 Satellite Imagery, *Civil and Environmental Engineering*, (June), U.S. Dep. Commer., NOAA Tech. Memo., NOAA-TM-NMFS-PIFSC, pp.24–46.

El-Asmar, H. and Hereher, M. (2011), "Change detection of the coastal zone east of the Nile Delta using remote sensing", *Environ Earth Sci* 62:769–777. <https://doi.org/10.1007/s12665-010-0564-9>

Elsahabi, M. A., Makboul, O., and Negm, A. M., "LAKE NUBIA BATHYMETRY DETECTION BY SATELLITE REMOTE SENSING", *International Water Technology Journal*, IWTJ, 2018, 8(1):9-17

ENVI, (2009).ENVI Atmospheric Correction Module: QUAC and FLAASH User's Guide, ITT Visual Information Solutions.

Gholamalifard, M., Kutser, T., Esmaili-Sari, A., Abkar, A.A., And Naimi, B., "Remotely Sensed Empirical Modeling of Bathymetry in the Southeastern Caspian Sea", *Remote Sensing Journal*, 2013, 5, 2746-2762; [DOI: 10.3390/rs5062746](https://doi.org/10.3390/rs5062746)

Green, E.P., Mumby, P. J., Edwards, A. J. and Clark, C. (1996). A Review of Remote Sensing for The Assessment and Management of Tropical Coastal Resources. *Coastal Management*, 24(1), pp.1–40.

Hedley JD, Harborne AR and Mumby PJ (2005) Technical note, "Simple and robust removal of sun glint for mapping shallow water benthos", *International Journal of Remote Sensing* 26(10): 2107–2112.

Hochberg, E.J., Andrefouet, S. and Tyler, M.R. (2003), "Sea Surface Correction Of High Spatial Resolution Ikonos Images To Improve Bottom Mapping In Near-Shore Environments", *IEEE Transactions on Geoscience and Remote Sensing* 41(7):1724–1729

Jagalingam, P., Akshaya, B.J. and Hegde, A.V. (2015), "Bathymetry Mapping Using Landsat-8 Imagery", *Procedia Engineering* 116:560-566.

Landsat 8 (L8) Data Users Handbook v.2, Department of the Interior U.S. Geological Survey, March 29, 2016, [landsat@usgs.gov](mailto:landsat@usgs.gov).

Leu, L. and Change, H. (2005), "Remote Sensing In Detecting The Water Depths And Bed Load Of Shallow Waters And Their Changes", *Ocean Engineering*, 32, 1174-1198.

Lyzenga DR (1985), " Shallow-water bathymetry using combined Lidar and passive multispectral scanner data", *Int J Remote Sens* 6(1):115–125. [Doi: 10.1080/01431168508948428](https://doi.org/10.1080/01431168508948428)

Makboul, O., Negm, A., Mesbah, S., Mohassab, M. (2018), "Assessment of Different Bathymetry Statistical Models Using Landsat-8 Multispectral Images", *Hydrologic Modeling, Water Science and Technology Library* 81:277-290, [https://doi.org/10.1007/978-981-10-5801-1\\_20](https://doi.org/10.1007/978-981-10-5801-1_20)

Melsheimer, C. and Chin, L.S. (2001) *Extracting Bathymetry From Multi-Temporal SPOT Images. Asian Conference on Remote Sensing*, 58(12), pp.37–42.

Mohammed, H., Negm, A.M., Salah, M., Nadaoka, K. (2017), "Assessment of Proposed Approaches for Bathymetry Calculations Using Multispectral Satellite Images in Shallow Coastal/Lake Areas: A Comparison of Five Models ", *Arab J Geosci*, p.p. 10-42, [Doi: 10.1007/s12517-016-2803-1](https://doi.org/10.1007/s12517-016-2803-1)

Negm, A.M., Msbah, S., Abdelaziz, T., and Makboul, O. (2017), "Nile River Bathymetry by Satellite Remote Sensing Case Study: Rosetta Branch", *the Nile River, Hdb Env Chem*. [DOI 10.1007/698\\_2017\\_17](https://doi.org/10.1007/698_2017_17)

Patel, A., Katiyar, S.K. and Prasad, V. (2015), "Bathymetric Mapping of Bhopal City Lower Lake Using IRS-P6:LISS-4 Imagery and Artificial Neural Network Technique", *J Indian Soc Remote Sens*. [DOI:10.1007/s12524-015-0523-8](https://doi.org/10.1007/s12524-015-0523-8)

Poppenga, S.K., Palaseanu-Lovejoy, M., Gesch, D.B., Danielson, J.J., And Tyler, D.J., 2018, "Evaluating The Potential For Near-Shore Bathymetry On The Majuro Atoll , Republic Of The Marshall Islands, Using Landsat 8 And Worldview-3 Imagery" : U.S. Geological Survey Scientific Investigations Report 2018-5024, 14 p., <https://doi.org/10.3133/sir20185024>.

Pushparaj, J. and Hegde, A.V., " Estimation of bathymetry along the coast of Mangaluru using Landsat-8 imagery", *The International Journal of Ocean and Climate Systems* 2017, Vol. 8(2) 71–83, <https://doi.org/10.1177/17593131166796>

Sánchez-Carnero N, Ojeda J, Rodríguez D, Marquez J (2014), "Assessment of different models for bathymetry calculation using SPOT multispectral images in a high-turbidity area", *the mouth of the Guadiana estuary. Int J Remote Sens* 35(2):493–514, [Doi:10.1080/01431161.2013.871402](https://doi.org/10.1080/01431161.2013.871402)

Stumpf R, Holderied K, Sinclair M (2003), " Determination of water depth with high-resolution satellite imagery over variable bottom types", *Limonology And Oceanography* 48:547–556. [doi:10.4319/lo.2003.48.1\\_part\\_2.0547](https://doi.org/10.4319/lo.2003.48.1_part_2.0547)

Su H, Liu H, Heyman W (2008), " Automated derivation of bathymetric information from multi-spectral satellite imagery using a non-linear inversion model", *Mar Geod* 31:281–298, [doi:10.1080/01490410802466652](https://doi.org/10.1080/01490410802466652)

Thompson, J. R., Flower, R. J., Ramdani, M., Ayache, F., Ahmed, M. H., Rasmussen, E. K. and Petersen, O. S., " Hydrological characteristics of three North African coastal lagoons: insights from the MELMARINA project" *Hydrobiologia* (2009) 622:45–84, [DOI 10.1007/s10750-008-9680-x](https://doi.org/10.1007/s10750-008-9680-x)

Todd U, Chris C (2010), " Radiometric use of WorldView-2 imagery technical note 1 WorldView-2 instrument description", Available on [http://global.digitalglobe.com/sites/default/files/Radiometric Use of WorldView-2 Imagery \(1\).pdf](http://global.digitalglobe.com/sites/default/files/Radiometric_Use_of_WorldView-2_Imagery_(1).pdf)

Zahran, M.A., El-Amier, Y.A., El nagger, A.A., Mohamed, H.A.and El-Alfy, M.A. (2015), "Assessment and distribution of heavy metals pollutants in Manzala Lake", Egypt. J Geosci Environ Prot 2015(3):107–122. <https://doi.org/10.4236/gep.2015.36017>